Journal of Cleaner Production 235 (2019) 1006–1019

Contents lists available at ScienceDirect

Journal of Cleaner Production

journal homepage: www.elsevier.com/locate/jclepro

Investigation of environmental, operational and economic performance of methanol partially premixed combustion at slow speed operation of a marine engine

Burak Zincir [a, *], Cengiz Deniz [a], Martin Tunér [b]

[a] Istanbul Technical University, Maritime Faculty, Postane Mah. Sahil Cad. Tuzla, 34940, Istanbul, Turkey
[b] Lund University, Department of Energy Sciences, Division of Combustion Engines, Lund, Scania, 221 00, Sweden

ARTICLE INFO

Article history:
Received 1 April 2019
Received in revised form
2 July 2019
Accepted 4 July 2019
Available online 9 July 2019

Handling editor: Giorgio Besagni

Keywords:
Methanol
Partially premixed combustion
Slow speed
Low load operation

ABSTRACT

This study aims to investigate the environmental, operational and economic performance of the methanol partially premixed combustion concept at slow speed operation of a ship to find a solution for the shipping emission effect on the coastal settlements while do not increase the risk and expense of the engine operation on the ships. The experimental study was done with partially premixed combustion, one of the advanced combustion concepts, on a Scania D13 heavy-duty diesel engine for its promising results of high engine efficiency and low engine emissions. In addition to the experimental study with methanol fuel, the performance of the methanol was compared with marine gas oil, which was mostly used at the slow speed operation of the ships. Empirical equations and coefficients in the literature were used to calculate specific fuel consumption, efficiency, and emissions of the marine gas oiled operation of the engine. The results showed that the combustion efficiency varied from 0.94 to 0.99 and the gross indicated efficiency varied from 0.42 to 0.46 from 10% to 25% engine loads, respectively, while the gross indicated efficiency of the marine gas oil-fuelled engine was 0.32 as a maximum value. The methanol showed good environmental performance with lower CO_2 emissions than the marine gas oil, lower NO_X emissions than the NO_X Tier III levels, varied between 0.3 g/kWh and 1.4 g/kWh, zero SO_X emissions and zero PM emissions. The economic investigation showed that the methanol cost at the low price scenario was 0.147 $/kWh, 0.138 $/kWh and 0.135 $/kWh at 10%, 15% and 25%, respectively, which were lower than the high price scenario and low price scenario of the marine gas oil; and the methanol high price scenario was still competitive with the marine gas oil scenarios.

1. Introduction

The transportation sector is an essential part of international trade, and the most important transportation type is sea transportation. Delivery of goods from one place to another place by sea transportation forms the 90% of the global trade (Deniz and Zincir, 2016), and almost 90% of external freight and 40% of internal freight of the European Union is carried by sea transportation (Fan et al., 2018). According to UNCTAD, the sea transportation has the fastest growth in five years with 4% annual growth in 2017 and reaches to 10.7 billion tons of cargo transportation by 94169 ships in various tonnages (UNCTAD, 2018). International Maritime Organization (IMO) states that all ships worldwide consume 300 million tons of fuel annually, and they emit 19 thousand tons of nitrogen oxide (NO_X) emissions, 10240 thousand tons of sulfur oxide (SO_X) emission, 938 million tons of carbon dioxide (CO_2) emissions, 1402 thousand tons of particulate matter (PM) emissions and 936 thousand tons of carbon monoxide (CO) emissions in 2012 (IMO, 2014).

Sea transportation can be done at open seas at normal speeds or reduced speeds. Slow speed navigation is done at the open seas as an emission reduction method, which is named as slow steaming. The slow steaming approach was firstly proposed by Maersk in 2007 as a fuel saving method (Tezdogan et al., 2015). The CO_2 emissions are the main target of the method, due to reduced total fuel consumption in a voyage. MAN B&W states that safe and reliable continuous slow steaming can be done at the engine operation down to a 10% engine load with the appropriate

* Corresponding author.
E-mail addresses: bzincir@itu.edu.tr (B. Zincir), denizc@itu.edu.tr (C. Deniz), martin.tuner@energy.lth.se (M. Tunér).

https://doi.org/10.1016/j.jclepro.2019.07.044
0959-6526/

precautions (Jensen and Jakobsen, 2009; MAN, 2012). Corbett et al. (2009), indicated at their study that the CO_2 emissions can be mitigated approximately 20–30% by the slow steaming approach. A constituted model showed that the slow steaming can reduce the CO_2 emissions from 1122 million tons per year to 804 million tons per year by 28% reduction without any abatement cost (Lindstad et al., 2011). Cariou (2011) made a study on the slow steaming application on a container ship group. He found that the CO_2 emissions are proportional to the consumed fuel, and the CO_2 emissions were reduced by around 11% over the past 2 years. Norlund and Gribkovskaia (2013) did a study on speed optimization in supply vessel operations. They reduced ship speeds at their study as a speed optimization technique. They achieved savings up to 25% in fuel consumption for the fleet, and an annual reduction of 900 tons of CO_2 emissions for a single vessel. A study was showed that the slow steaming reduced power requirements, fuel consumption and CO_2 emissions (Tezdogan et al., 2016). The slow steaming approach can decrease up to 53% at a ship's effective power and CO_2 emissions. Another study was done to investigate the CO_2 emission reduction of the slow steaming at a RO-RO cargo vessel by a case study (Ammar, 2018). It was found that the CO_2 emissions reduced by 27.1% and 78.4% at a ship speed reduction of 10% and 40%, respectively.

Other slow speed navigation execution areas are straits and canals. These areas are more dangerous and risky areas, which are close to the coast and shallow waters. It is essential that the stable operation of the main engine at slow speed low load operation is needed at these areas to prevent undesirable incidents. According to the data of the study, the slow speed low load operation of the main engine of the ships is approximately 20% of all loads of the main engine (Baldi et al., 2013). Another study indicates that container ships navigate up to 20% load of the main engine at 18% of their operational profile, while RO-RO and passenger ships navigate 20% and 23% of their operational profile, respectively (Jafarzadeh and Schjølberg, 2018).

Besides the stable operation of the main engine, the effects of the shipboard emissions on coastal settlements are another issue. Especially, the NO_X emission and, SO_X emission, which are the reason of acid rains, the PM emissions, which are the reason of deterioration of air quality, and black carbon (BC) emission (Janssen et al., 2012), which is the reason of degradation of vegetation areas, are important emission types are emitted from ships to the coastal settlements. There are various studies about the emission levels of port areas, which is an indicator of the coastal emission effects of shipping. These studies belongs to Deniz and Durmusoglu (2008) at the Sea of Marmara; Deniz and Kilic (2010) at Ambarli Port; Merico et al. (2017) at Brindisi, Venice, Patras and Rijeka ports; Styhre et al. (2017) at Gothenburg, Long Beach, Osaka and Sydney ports; Dragovic et al. (2018) at Dubrovnik and Kotor ports. The health impacts of ship emissions at five Greek ports for the year 2013 was investigated in a study (Maragkogiannia and Papaefthimiou, 2015). They found that the health impact costs can reach to 24.3 million € per year. Another study indicated that the overall external cost in health caused by air pollutants emitted by the passenger ships at Piraeus port is 26 million € (Chatzinikolaou et al., 2015).

In addition to the slow steaming approach, there are various emission abatement methods for the pollutants. Some of these methods are exhaust gas recirculation (EGR), water injection to the combustion chamber, selective catalytic reduction (SCR), SO_X scrubbers, etc. As well as these methods, the usage of alternative fuels for ships is a trend emission abatement method. The engine efficiency can be increased or remained constant, and all type of emissions can be decreased simultaneously while existing emission abatement methods have a negative effect on the engine efficiency and cannot reduce all emissions with one type of emission abatement method. Lower carbon fuels and no sulfur fuels are preferred to reduce shipboard emissions. Some of these fuels are liquefied natural gas (LNG), liquefied petroleum gas (LPG), methanol (MeOH) and ethane. Worldwide alternative fuelled ship numbers are 116 LNG, 12 LPG, 2 methanol and 2 ethane fuelled ships. Additionally, there are 112 and 6 confirmed new buildings for LNG and methanol, respectively (Zincir and Deniz, 2018).

Even if the MeOH fuelled ships are low in numbers, there are various studies and projects with the methanol fuel, increasing its popularity day by day. Some of the maritime-based projects with MeOH fuel are Effship, Spireth, Methaship, Leanships, Summeth, and Greenpilot (Ellis, 2017). The MeOH is the simplest alcohol that can be produced from both renewable and fossil fuel sources, for instance, natural gas, coal, wood, agricultural and municipal waste, etc. (Yao et al., 2017). It has a higher H/C ratio than the conventional fuels. In addition to this, the MeOH has high oxygen content and high octane number (ON). This high oxygen content assists more efficient combustion. The greenhouse gases are reduced (Shahhosseini et al., 2018), and no SO_X emissions are formed with MeOH combustion. The NO_X and soot emissions are low, due to lowered in-cylinder gas temperature by the MeOH combustion (Wei et al., 2015; Pan et al., 2015; Gong et al., 2018). Low-temperature combustion also reduces the heat transfer loss, and the high latent heat of vaporization lessens the compression work, both resulting in higher engine efficiency (Shamun et al., 2018).

In normal conditions, the MeOH cannot be burned in compression ignition engines, due to its high octane number (ON), which shows high resistance of the fuel to auto-ignition. It can be combusted by pilot diesel fuel in dual-fuel combustion concept, by spark plug in direct injection spark ignition (DISI) combustion concept or by using partially premixed combustion (PPC) concept. The PPC is an intermediate process of the conventional diesel combustion and homogenous charge compression ignition (HCCI) combustion. The direct injection event and auto-ignition event are separated at the PPC concept (Tuner, 2016). Fuel is injected at a crank angle during the compression stroke, which aims to form a partially homogenous mixture with air, residual gases and fuel. Benajes et al. (2014), investigated the performance of the PPC concept using commercial gasoline with RON95 in their newly designed 2-stroke poppet valves diesel engine. The engine was operated at 5 bar IMEP at 1200 rpm with the combustion stability of 3% and combustion efficiency of 98%. Han et al. (2017), did a study to evaluate the advantages and disadvantages of using neat n-butanol in a diesel engine with the PPC concept at around 6 bar of IMEP. They observed that the indicated thermal efficiencies were 45.3% and 45.4% for n-butanol and diesel, respectively. Lower reactivity and less complete burning of the n-butanol slightly reduced the combustion efficiency. It was indicated that the n-butanol had lower NO_X and near to zero smoke emissions. The previous study of Shamun et al. (2018), investigated the charge cooling effect of the methanol. It was observed that the charge cooling effect slightly reduced the compression work, and in the expansion stroke, during the combustion, the charge cooling effect had existed highly. The methanol reduced the heat transfer loss, which resulted in higher engine efficiency. Yin et al. (2019a), investigated the effects of the calibration parameters of the PPC on the efficiency and emissions of a multi-cylinder engine during stable and transient operations at 5, 11 and 14 bar loads. Experiment fuel is a mixture of 80% Swedish 95 octane pump gasoline and 20% n-Heptane. They observed that the peak gross indicated efficiency was 51.5% and the peak net indicated efficiency was 48.7% at stable operating conditions. The transient condition had a 47.5% average net indicated efficiency. It was also indicated that the NO_X emissions, CO emissions, and THC emissions comply with the Euro VI emission limits at almost all transient operating conditions.

There are some other PPC studies in the literature and detailed information about the effect of the PPC concept on the engine performance and the emissions can be found at the studies of Leermakers et al. (2014), Jain et al. (2017), Naser et al., (2017), Wang et al. (2017), Mao et al. (2018), An et al. (2018), An et al. (2019) and Yin et al. (2019b).

The interest in MeOH has been increased lately, due to its unique combustion properties. Furthermore, the PPC concept, one of the advanced combustion concepts, has promising results of high efficiency and low emissions for cleaner engine operation. Using MeOH under the PPC concept can be a possible future solution for the shipping emission effect on the coastal settlements while it does not increase the risk and expense of the engine operation. Although there are some studies in the literature with the MeOH fuel usage on ships, these studies focus on fuel consumption, emissions, and fuel expenses at full load operation of the engine by using empirical or theoretical equations in the literature to calculate the fuel consumption and emissions. There is a gap in the literature about the slow speed low load operation of a ship and detailed experimental investigation of the MeOH fuelled operation. Another gap is a lack of studies and knowledge about the MeOH PPC concept and its application with the maritime industry. The increasing importance of the slow speed navigation, unique characteristics of the MeOH fuel and the PPC concept are the motivations of this study. In this study, the low load operation from a 10%–25% engine load under the MeOH PPC concept is experimentally investigated. The MeOH fuelled engine operation is examined by considering the combustion stability, maximum pressure rise rate, in-cylinder, and exhaust temperatures and engine efficiencies. The specific fuel consumption (SFC), emissions of CO_2, NO_X, SO_X, PM, CO and THC, and fuel cost are discussed. The experimental findings of MeOH PPC are compared with the empirical formula calculation results of the marine gas oil (MGO) to observe the advantages of the MeOH PPC concept over conventional MGO combustion. The SFC, efficiency, and emission results of the MeOH are gathered from the experimental studies, while they are calculated by the empirical equations in the literature for the MGO.

2. Methodology

This study included experimental and calculation parts and two types of fuels were the subjects of the study. These fuels are methanol (MeOH) and marine gas oil (MGO). The MeOH was specifically selected for the unique properties of the fuel, while the MGO was selected because it has to be used for ship's slow speed operation, such as canal and strait passages, coastal navigation, etc., to comply with IMO and port state emission rules and regulations.

2.1. Experimental setup

The experimental part was done to observe the effect of the MeOH PPC application on the operational performance and environmental performance at the slow speed low load operation of the engine. The study was done at the laboratory of the Division of Combustion Engines, Department of Energy Sciences at Lund University. The engine which was used at the experimental study is a six-cylinder Scania D13 heavy-duty engine modified to run only one cylinder. Specifications of the engine are shown in Table 1.

Fig. 1 and Fig. 2 show the experimental setup of the test rig and Table 2 shows the specification of the sensors used in the engine test cell. Pressurized air is delivered from an external compressor, and the back pressure of turbocharger can be simulated by the back pressure valve. The back pressure valve was not used in this study, since no boosting was applied. The 7.5 kW air heater at the intake air line was used for the heating of the intake air in this study.

Table 1
Engine specifications.

Engine Specifications	
V_d	2124 cm^3
Stroke	160 mm
Bore	130 mm
r_c	17.3
Swirl ratio	2:1
IVC	−141 CAD ATDC
EVO	137 CAD ATDC
Umbrella angle	148°
Injector type	10 hole MeOH injector
Rated speed	2100 rpm
Rated power (single cylinder)	~49 kW

The crank angle of the engine was detected by a Kistler 2614CK crank angle encoder located on the crankshaft. The encoder sends two signals. The first one is for a high sampling frequency of the crank angle at every 0.2°CA and the second signal is for sampling completed engine revolutions for engine speed calculation. The in-cylinder pressure was measured by a Kistler 7061B piezoelectric pressure sensor. It sends an electric charge signal to a Kistler 5011 charge amplifier. Gross indicated mean effective pressure (IMEP) and net indicated mean effective pressure ($IMEP_n$) was calculated according to the pressure measurements.

The heat release rate was calculated by the use of the measured cylinder pressure. The apparent heat release rate (aHRR) equation is (1), while the ratio of specific heats (γ) is calculated with equation (2). The IMEP and the $IMEP_n$ are calculated with equations (3) and (4), respectively by using measured cylinder pressures.

$$dQ_{hr} = \gamma/(\gamma-1)\ .P\ .\ dV + 1/(\gamma-1)\ .V\ .dP \tag{1}$$

$$\gamma = C_p/C_v \tag{2}$$

$$IMEP = 1/V_d \int_0^{360} p\ dV \tag{3}$$

$$IMEP_n = 1/V_d \int_0^{720} p\ dV \tag{4}$$

The coefficient of variation of $IMEP_n$ (COV $IMEP_n$) was derived from the cylinder pressure signal, and the start of combustion, combustion angles (CA10, CA50, CA90), ignition delay was determined from the calculated rate of heat release (RoHR). The experimental data were gathered by saving three sampling periods for each operating point, each of these sampling periods included 300 consecutive cycles. The mean value of these 900 cycles for every operating point was used in the results section.

Emissions of CO, THC, and NO_X were measured by Horiba Mexa 7500 DEGR. An IRD (infrared detector) method is used to measure the CO, whereas a CLD (Chemiluminescence detector) is used to measure the NO_X and NO, while a FID (Flame ionization detector) is for THC measurement. The MeOH fuel is a sulfur-free fuel, for this reason, the SO_X emissions were not investigated. Also, PM emissions were not investigated, due to the low emission amount always encountered (Shamun et al., 2017).

2.2. Test fuel

The fuel used in the study was chemical grade MeOH which had a purity of 99.85%. Water and trace amount of organic compounds

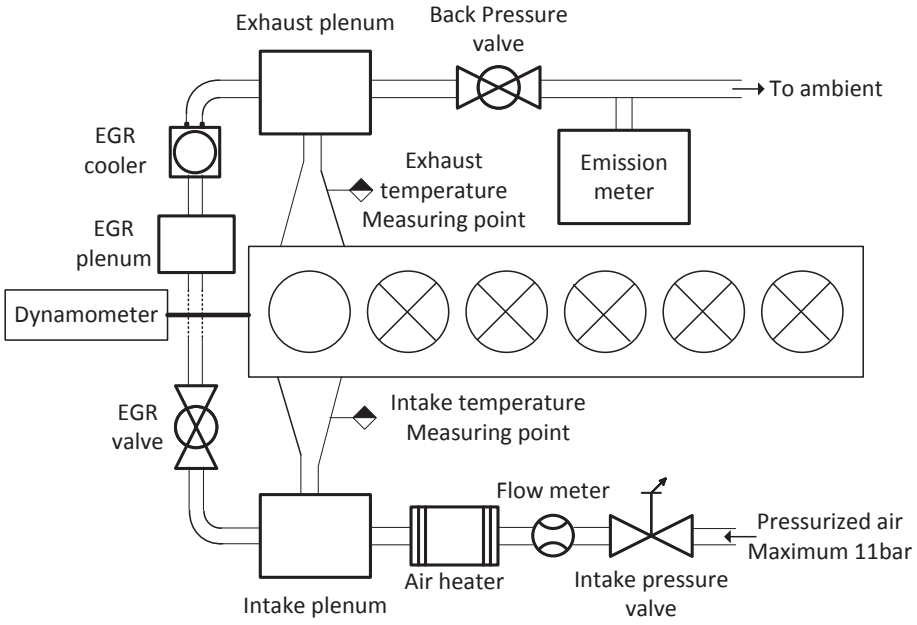

Fig. 1. Experimental setup diagram.

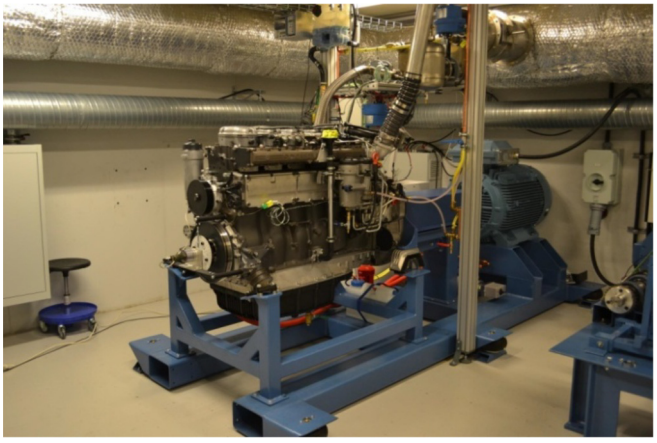

Fig. 2. Picture of the experimental setup.

constituted the remaining content. The properties of the MeOH can be seen in Table 3. To improve the lubricity, a small amount, 200 ppm, of Infineum R655 was mixed to the MeOH. It has near to zero effect on the combustion and combustion products. The energy density of the additive was neglected in the experiment.

Table 3
Properties of methanol (Shamun et al., 2016).

Specifications	Methanol
RON	107–109
MON	92
H/C	4
O/C	1
LHV [MJ/kg]	19,9
A/F_s	6,45
Density [kg/m^3]	792
Heat of Vaporization [kJ/kg]	1103

2.3. Test procedure

According to IMO (2014), the engine load of a ship at maneuvering is the load which provides the ship sails with greater than 3 knots and less than 20% maximum continuous rating (MCR) of a ship. On the other side, the slow steaming can be done at the engine load below to 10% MCR (Jensen and Jakobsen, 2009). Under the light of this information, the engine was operated at the IMEP of 2 bar, 3 bar and 5 bar at 800 rpm, which represented 10%, 15% and

Table 2
Specification of sensors used in the engine test cell.

Sensor	Model	Measurement Range	Precision
CA Encoder	Kistler 2614CK	0–12000 rpm	±0.03°CA
Cylinder Pressure	Kistler 7061B	0–250 bar	
	Kistler 5011		
Intake Manifold Pressure	Kistler 4075A10	0–10 bar	±0.03% FS
Exhaust Manifold Pressure	Kistler 4075A10	0–10 bar	±0.03% FS
Fuel Injection Pressure	Kistler 4067C	0–3000 bar	±0.5% FS
Air Flow Meter	MicroMotion 1700	0–725 kg/min	±0.1% FS
Fuel Flow Meter	Vettek APP 25.R2	0-25000 gr	±0.1 gr
O_2	ETAS ES630.1	0–25%	
CO	Horiba	0–10000 ppm	±1% FS
NO_X	MEXA7500DEGR	0–1000 ppm	±1% FS
THC		0–4000 ppm	±1% FS
O_2		0–25%	±1% FS

25% engine loads, respectively. Table 4 shows the engine test parameters during the experiments. The injection pressure was 400 bar, and the start of injection (SOI) was −18, −28, −40 ATDC at 10%, 15% and 25% engine loads, respectively. The SOI timings are determined by the purpose of holding the crank angle where half of the heat is released at 5°CA (CA50) at all operated loads. The intake temperature was constant at 150 °C at all operating loads for the good combustion of the MeOH by reducing its resistance to the auto-ignition while applying the PPC concept.

2.4. Calculations

The second part of the study is the calculations part. The experimental part of the study is done with MeOH fuel. Since the MGO fuel is not used in the experimental studies, the empirical and theoretical equations are used to calculate the SFC, emissions, and efficiency of the MGO fuelled engine. Besides the equations for the MGO fuel, there are equations just for the MeOH or for both fuels, which are explained in the sub-sections.

2.4.1. Emission calculations

Specific emissions of the MGO fuel are not measured, because there is no experimental study done with this fuel in this study. The specific emissions of MGO fuel for the low loads are calculated by equations (5) and (6) (Ammar, 2019; Ammar and Seddiek, 2017; EEA, 2000), and emission factor coefficients in Table 7 (Ammar, 2019; Ammar and Seddiek, 2017; ICF, 2009) are used in the equations.

$$E = a(\%load)^{-z} + b \tag{5}$$

$$E_{SOx} = a(SFC\ x\ S\%) + b \tag{6}$$

Where a, z and b are coefficients for the emission factors. S% is the fuel sulfur fraction, which is 0.1%, which represents low sulfur marine gas oil (LSMGO).

Specific emissions from MeOH for the low loads are calculated based on the experimental studies, except CO_2 emissions. The emissions of CO_2 are calculated according to equation (7), which is the same as the CO_2 emission calculation of IMO;

$$f_{CO2} = f_C\ x\ (m_{CO2} / m_C) \tag{7}$$

Where f_c is the carbon content of MeOH, is 0.375; m_{CO2} is mass of CO_2 after stoichiometric combustion of MeOH, and m_C is mass of carbon in MeOH. The CO_2 emission factor is found as 1.375, which is consistent with the study of Gilbert et al. (2018).

2.4.2. Combustion stability calculation

The combustion stability calculation is just made for the MeOH fuel. The COV $IMEP_n$ is the indicator of combustion stability. The calculations of the COV $IMEP_n$ were made by equations (4), (8) and (9).

$$\overline{x} = 1/N \sum_{1}^{N} x_i \tag{8}$$

$$COV\ IMEP_n = \left(\sqrt{\sum_{i=1}^{N} (x_i - \overline{x})^2 / N} \right) \Big/ \overline{x}\ 100\% \tag{9}$$

Where N is consecutive sampled cycles at the experiments (N = 300), and x_i is $IMEP_n$ of a specific combustion cycle.

2.4.3. Specific fuel consumption and specific energy consumption calculations

The specific fuel consumption (SFC) of the main engine at the low load operation is higher than the maximum continuous rating of the engine, due to reduced engine efficiency. For this reason, there is a specific empirical equation for the SFC calculation at the low load engine operation with conventional fuels (Ammar and Seddiek, 2017; EEA, 2000). The SFC of MGO is calculated by equation (10), while it is got from the experimental study for MeOH.

The specific energy consumption (SEC) of the main engine under MeOH and MGO fuel operation is calculated by equation (11) in MJ/kWh basis. The LHV of MeOH is used as 19.9 MJ/kg, while the LHV of MGO is used as 42.8 MJ/kg at the SEC calculation (ETB, 2003).

$$SFC = 14.1205\ /\ \%load\ +\ 205.7169 \tag{10}$$

$$SEC = (SFC\ x\ LHV)/\ 1000 \tag{11}$$

2.4.4. Efficiency calculations

The combustion efficiency (η_c), the thermodynamic efficiency (η_t) and the gross indicated efficiency (η_{GIE}) of the MeOH fuel are investigated in this study. The efficiencies are calculated by the equations from (12) to (14).

$$\eta_c = QMEP\ /\ FuelMEP \tag{12}$$

$$\eta_t = IMEP\ /\ QMEP \tag{13}$$

$$\eta_{GIE} = IMEP\ /\ FuelMEP \tag{14}$$

Where QMEP is the heat of the burned fuel and FuelMEP is the total fuel energy.

Although the operating conditions of the MGO fuelled diesel engine at the low load operation are not known, it is possible to calculate rough engine efficiency to compare with the MeOH fuelled engine operation. Equation (15) is used to calculate the η_{GIE} of the MGO fuelled engine operation (Klaus et al., 2013).

$$\eta_{GIE_{MGO}} = 3600/(LHV\ x\ SFC) \tag{15}$$

2.4.5. Fuel cost calculation

Fuel cost for MeOH and MGO is calculated by equation (16) in a usd/kWh basis.

Table 4
Engine test parameters.

Engine Load			
Engine Parameters	10%	15%	25%
IMEP [bar]	2	3	5
Engine Speed [RPM]	800	800	800
Injection pressure [bar]	400	400	400
Start of injection [CAD]	−18	−28	−40
Injection duration [μs]	1100	1310	2170
Intake temperature [°C]	150	150	150
Intake pressure [bar]	1	1	1
Coolant temperature [°C]	85	85	85
EGR [%]	0	0	0
λ	4.3	3.4	2.2

$$FP_i = SFC_{ji} \times FC_j / 10^6 \quad (16)$$

Where FP_i is the fuel cost at i engine load, SFC_{ji} is the specific fuel consumption of j type of fuel at i engine load and FC_j is the cost of j type of fuel per metric ton.

3. Results and discussions

According to the study of Dere and Deniz (2019), the fuel consumption, generated emissions, combustion parameters, such as the combustion temperatures and combustion pressures decrease with low load operation of the engine. This section investigates these issues at the environmental performance and operational performance sub-sections by comparison with the MGO fuel to observe the advantages of the MeOH fuelled engine. In addition, the economic performance of the MeOH and MGO fuels at low load operation is calculated. The MGO results are obtained by the equations in the literature related to conventional diesel combustion, while they are attained from the PPC experiments for MeOH.

3.1. Environmental performance

Shipboard emissions are an important issue for the maritime industry. Rules and regulations for the emission reduction at shipping are becoming stricter day by day. In addition to the reduced worldwide emission limits, there are Emission Control Areas (ECA), includes important ports and trade routes are the Pacific coasts of U.S., the Atlantic coasts of U.S., Canada, Gulf of Mexico coast of the U.S., Caribbean Sea, the Baltic Sea and the North Sea (IMO web, 2019a), which are the areas that the emission limits are lower than the global emission limits. This means if the ships do not comply with the ECA emission limits, they cannot do navigation at these areas and results in trade area limitation and money loss.

Section 3.1.1 gives information about the emission rules and regulations at the maritime industry, and section 3.1.2 includes results and comments about the low load engine operation with the MGO and MeOH fuels.

3.1.1. Shipping emission rules and regulations

CO_2, NO_X, SO_X and PM emissions are the regulated emissions for shipping. The CO_2 emissions are one of the important greenhouse gas and the highest amount of emission type from the combustion of the fuels. The CO_2 emissions have been regulated by the Regulations on Energy Efficiency for Ships in MARPOL Annex VI which was entered into force by IMO on 1 January 2013 (IMO, 2011). It aims to control and mitigate CO_2 emissions from ships. Energy Efficiency Design Index (EEDI) for new building ships and the Ship Energy Efficiency Management Plan (SEEMP) for existing ships were defined with the regulation. On 1 July 2015, the EU MRV (Monitoring, Reporting, Verification) regulation entered into force by European Union countries, Norway and Iceland (DNV GL, 2016). This regulation aims to monitor, report and verify annual CO_2 emissions from ships larger than 5000 gross tonnages calling at any EU and EFTA (Norway and Iceland) ports. The fuel consumption data collection has started from 1 January 2018, and the CO_2 emissions have been calculated by the multiplication of a coefficient. Recent regulation, which is entered into force on 1 March 2018, is amendments to MARPOL Annex VI on Data Collection System for fuel oil consumption of ships adopted by the resolution MEPC.278(70) (IMO web, 2019b). It has the same aim as the MRV Regulation, but it is for the ships larger than 5000 gross tonnages calling at any worldwide ports.

The NO_X emissions are limited by the NO_X Technical Code – Regulation 13 of MARPOL Annex VI. This code is applied for all ships which have the engine power over 130 kW. There are three limitation tiers vary at different engine speed. Table 5 shows the NO_X limits for different tier levels and engine speeds (IMO web, 2019c). Tier III is applied at only ECAs, while Tier II is applied outside of the ECAs.

Table 5
NO_X emission limits.

Tier	Ship construction date on or after	Total weighted cycle emission limit (g/kWh) n = engine's rated speed (rpm)		
		n < 130	n = 130–1999	n ≥ 2000
I	1 January 2000	17.0	$45.n^{(-0.2)}$	9.8
II	1 January 2011	14.4	$44.n^{(-0.23)}$	7.7
III	1 January 2016	3.4	$9.n^{(-0.2)}$	2.0

The SO_X and PM emissions are limited by limiting the fuel sulfur content. There are different limitations for ECAs and non-ECAs. Table 6 shows the sulfur limits of the fuels (IMO web, 2019d).

3.1.2. Specific emissions

In this sub-section, the specific CO_2, NO_X, SO_X, PM, CO, and THC emissions of the MeOH and MGO fuels are compared. The CO_2 emission of the MeOH is found by the CO_2 emission factor, which is calculated by equation (7). On the other hand, CO_2 emission of the MGO is found by using equation (5) and the coefficients in Table 7. The specific emissions of NO_X, CO, and THC of MeOH fuelled engines are gathered from the experimental studies while these specific emissions, SO_X, and PM are calculated by using equation (5) and the coefficients at Table 7 for the MGO fuelled operation.

3.1.2.1. CO_2 emissions. The specific CO_2 emissions at the low load operation are shown in Fig. 3. It is observed that the MeOH fuel has lower CO_2 emission than the MGO. However the SFC of the MeOH is higher than the MGO, the carbon content of the MeOH is much lower than the conventional fuels and it results with lower CO_2 emissions. The MeOH has the carbon content of 37.5% while it is 85.7% for the MGO (GCS, 2019). In addition to this, the experimental studies with MeOH PPC showed that the engine efficiency using MeOH fuel is higher than the engine efficiency which is calculated by equation (15) for the MGO fuel operation. The engine efficiency is directly related to CO_2 emission that is mentioned at the previous sub-section. It is also seen that the CO_2 emissions decrease with the increase of the engine load, due to reduced fuel consumption. The MeOH fuel usage on ships has an advantage at the MRV and IMO Data Collection System regulations. The combustion of the MeOH results with lower CO_2 emission per ton cargo – nautical mile distance.

Most MeOH is produced from natural gas and coal however, it can also be produced from the biogenic feedstock. This type of MeOH is called as bio-methanol, and it is carbon neutral fuel. Another MeOH production method is done by using electricity from renewable energies and carbon capture from the atmosphere or waste CO_2. This type of MeOH is termed as electrofuel (Verhelst et al., 2019). This type of MeOH means instead of emitting additional CO_2 emissions to the atmosphere, it is in the constant environmental carbon cycle.

3.1.2.2. NO_X emissions. The specific NO_X emissions at the low load operation are shown in Fig. 4. The tier limits at 800 rpm of the engine speed are also shown in the figure as 11.8 g/kWh, 9.5 g/kWh and 2.4 g/kWh for Tier I, II and III, respectively. The specific NO_X emissions of the MGO reduces from 14.4 g/kWh to 11.5 g/kWh according to the calculations at 10% engine load to 25% engine load. It

Table 6
Fuel sulfur limits.

Outside ECA SO_X and PM Limits	Inside ECA SO_X and PM Limits
4.50% m/m prior to 1 January 2012	1.50% m/m prior to 1 July 2010
3.50% m/m on and after 1 January 2012	1.00% m/m on and after 1 July 2010
0.50% m/m on and after 1 January 2020	0.10% m/m on and after 1 January 2020

Table 7
Emission factor coefficients for main engine at low load.

Coefficient	NO_X	SO_X	PM	CO_2	CO	THC
a	0.1255	2.3735	0.0059	44.1	0.8378	0.0667
z	1.5	n/a	1.5	1.0	1.0	1.5
b	10.4496	−0.4792	0.2551	648.6	0.1548	0.3859

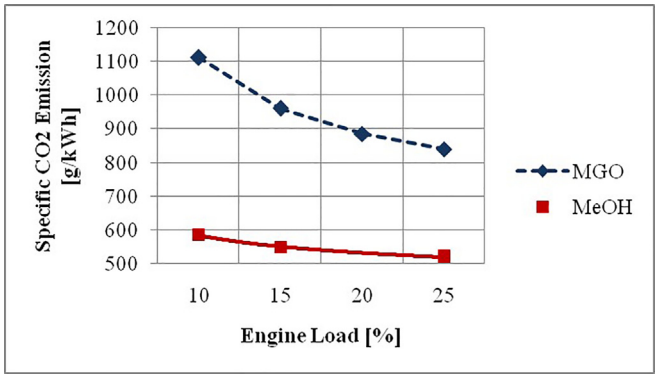

Fig. 3. Specific CO_2 emissions at low loads.

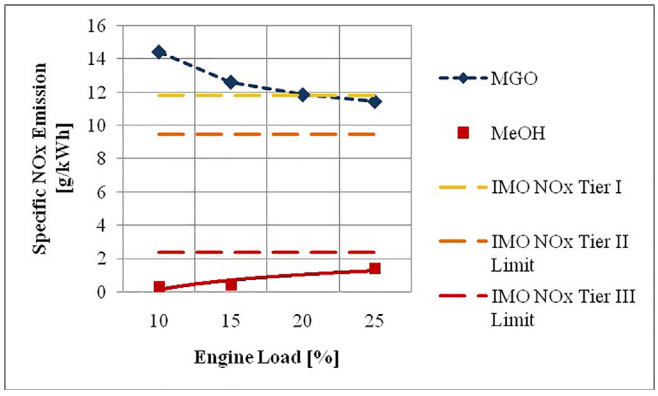

Fig. 4. Specific NO_X emissions at low loads.

can be seen that the NO_X emissions at the low load operation with the MGO fuel cannot comply with Tier II and III limits, and it only complies with Tier I limit above 20% engine load. It means after-treatment methods are needed to reduce NO_X emissions to the Tier II and Tier III limits to comply with the regulations while doing slow steaming or slow speed low load navigation.

The specific NO_X emissions of the MeOH PPC increases slightly from 0.3 g/kWh to 1.4 g/kWh at 10% engine load to 25% engine load, according to the experimental results. It is observed that the NO_X emission amount is under the IMO NO_X Tier III Limit. The results are consistent with the comments at the study (Brynolf et al., 2014). The higher latent heat of vaporization and high amount of injected fuel in the cylinder results with low combustion temperature and reduced NO_X emissions (Shamun et al., 2018). The MeOH PPC applied ships can sail in the ECAs while doing slow steaming approach or navigating at the slow speed near coastal areas.

3.1.2.3. SO_X emissions. Fig. 5 shows the specific SO_X emissions at the low load operation. The SO_X emission limits for ECAs and non-ECAs are calculated by the multiplication of allowable maximum sulfur limits (m/m) with SFC (g/kWh). The maximum allowable sulfur limits in the fuel are taken as 0.5% and 0.1% for non-ECAs and ECAs, respectively. The SO_X emissions of the MGO are calculated by equation (6). The MGO is assumed as low sulfur MGO (LSMGO), which has 0.1% sulfur in the fuel. According to the calculations, the specific SO_X emissions of the LSMGO is 0.34 g/kWh, 0.23 g/kWh, 0.18 g/kWh and 0.14 g/kWh at 10%, 15%, 20% and 25% engine load, respectively. The specific SO_X emissions at the low load are under the limit for ECAs. The MeOH is sulfur-free fuel, for this reason, the SO_X emissions of the MeOH PPC is assumed as zero in this study, the same as the study of Gilbert et al. (2018). As a consequence, it is naturally ECA compliant fuel.

3.1.2.4. PM emissions. Fig. 6 shows specific PM emissions at the low load operation. The PM emission ECA and non-ECA limits are the same as the SO_X emission limits. However, the MGO complies with the SO_X ECA limits; the PM emissions are slightly higher than the ECA limits. It is 0.44 g/kWh, 0.36 g/kWh, 0.32 g/kWh and 0.30 g/kWh according to the calculations at 10%, 15%, 20% and 25% engine load, respectively. The MeOH fuel emits almost zero PM emissions. According to the study, the emitted PM emissions are mainly from the lubrication oil rather than the combustion of the methanol (Shamun et al., 2017). The PM emissions were measured as 0.000004 g/kWh at another study (Tuner et al., 2018). For this reason, the PM emissions were assumed as zero in this study.

3.1.2.5. CO emissions. Although CO is not a regulated emission in shipping, CO is an indicator of the partial oxidation of the fuel during the combustion event. The CO emissions depend on the fuel/air equivalence ratio in the cylinder (Heywood, 1988). Fuel rich and fuel lean zones in the cylinder determine the amount of the CO formation. The CO emissions from the MGO and MeOH are shown in Fig. 7. It is calculated that the CO emissions of the MGO are

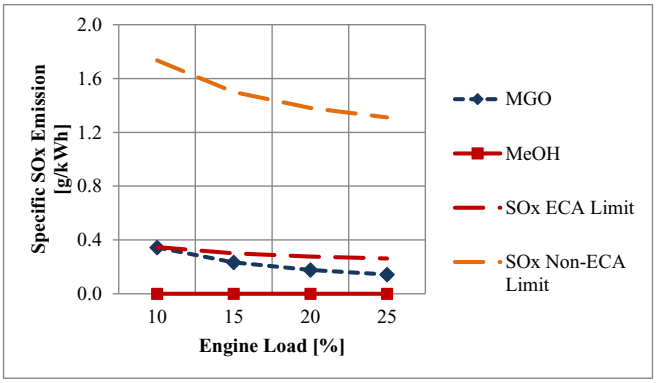

Fig. 5. Specific SO_X emissions at low loads.

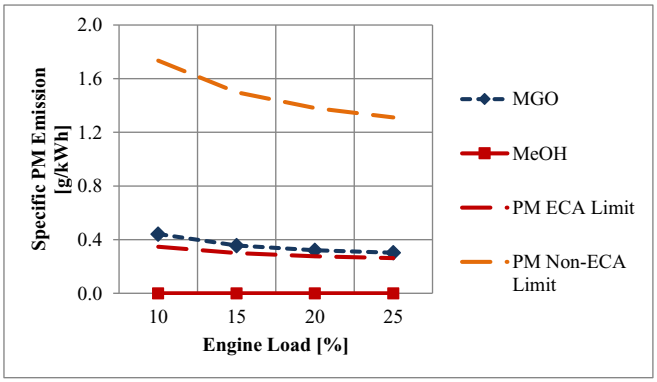

Fig. 6. Specific PM emissions at low loads.

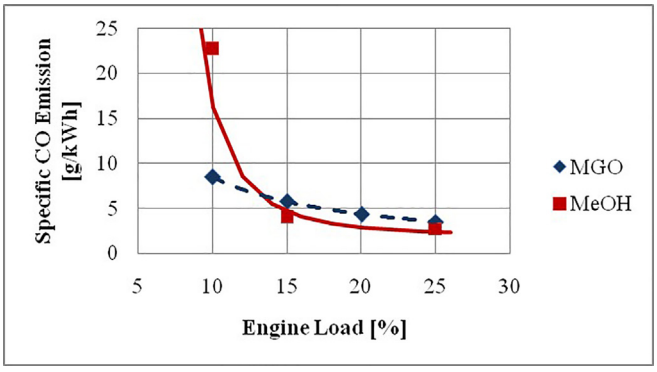

Fig. 7. Specific CO emissions at low loads.

reduced with the increase of the load from 10% to 25%. It is between 8.5 g/kWh and 3.5 g/kWh at the investigated load range. According to the experimental study, the CO emissions of the MeOH PPC are extremely much higher than the MGO with 22.7 g/kWh at a 10% engine load. The reason can be shorter ignition delay duration than higher loads that forms larger fuel rich zones and oxidation of the fuel does not adequate. In addition to this, the low engine speed can stop the CO oxidation into CO_2, due to the cooling down of the combustion mixture lower than the required temperature of 1500 K during the expansion stroke (Shamun, 2019; Sjöberg and Dec 2003). The CO emissions reduce to 4 g/kWh at 15% engine load and 2.7 g/kWh at 25% engine load, which are lower than the MGO at 15% and 25% engine loads.

3.1.2.6. THC emissions. The THC emissions are also one of the unregulated emissions, but they show incomplete combustion during operation. Crevice losses, over-leaning, under-mixing, colder in-cylinder temperature and cylinder walls are the reasons of THC emissions (Heywood, 1988). Fig. 8 shows the specific THC emissions of the MGO and MeOH fuels at the low load operation. It is observed that the THC emissions of the MGO are higher than the MeOH at almost all investigated loads, except at 25% load. The THC emissions of the MGO according to the calculations are 2.5 g/kWh, 1.5 g/kWh, 1.1 g/kWh and 0.9 g/kWh at 10%, 15%, 20% and 25% engine loads, respectively. The MeOH PPC has the THC emissions of 1.4 g/kWh, 0.8 g/kWh and 1.1 g/kWh at 10%, 15% and 25% engine loads, respectively. The in-cylinder temperatures are low under the low load operations, but heated intake air temperature to 150 °C can promote the combustion, reduce the resistance to ignite of the MeOH, and results in more complete combustion than the MGO combustion. THC emission firstly decreases and then increases by

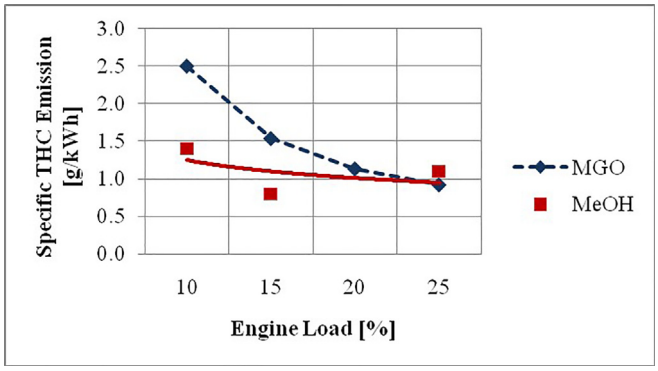

Fig. 8. Specific THC emissions at low loads.

the increase of the engine load. The SOI timing can affect THC emission. It is at −18°CA at a 10% engine load, but it is advanced to −40°CA at a 25% engine load to hold the combustion event at the same crank angle at each operating condition. This can lead to higher crevice losses which result in higher THC emission at 25% engine load than 15% engine load.

3.2. Operational performance

The engine operation of the MeOH is investigated by considering the combustion stability, maximum pressure rise rate, in-cylinder temperatures, and exhaust temperature and efficiencies of the engine at the low load operation.

In-cylinder pressures and RoHR curves from %10 engine load to %25 engine load are shown in Fig. 9. It is observed that the maximum in-cylinder pressure is increased with the increase of the engine load. It is close to 60 bar at a 10% engine load while it is at 75 bar at %25 engine load. The in-cylinder pressure curve is stepper with the raising engine load. The reason can be the SOI timing which affects the in-cylinder pressure trend. The SOI timings are determined by the purpose of holding the crank angle where half of the heat is released at 5°CA (CA50) at all operated loads. The RoHR curves show that the released heat is increased and the shape of the curve is narrower at higher engine loads. It means that the combustion event of the MeOH is quicker and the burn duration is reduced at higher engine loads.

3.2.1. Combustion stability

The combustion stability at low load operation of the diesel engines with conventional HFO and MGO fuels are well known for years. These fuels have high cetane number, which promotes auto-ignition, and as a consequence easier combustion even at low in-cylinder temperatures at low load operation. For this reason, the investigation of the combustion stability of the MGO is not done in this study. Combustion stability is an important parameter for the continuous smooth operation of a diesel engine. The engine stability was obtained from the calculation of COV $IMEP_n$. It is a criterion for combustion stability, and the upper limit of the COV $IMEP_n$ for engine stability is 5% (Przybyla et al., 2016). Above this limit, the variation of the produced power of the diesel engine increases, and it affects continuous operation of the engine. If the COV $IMEP_n$ is above 10%, the misfire starts to occur, and it is unacceptable for the continuous engine stability (Heywood, 1988). It is more important for high octane number fuels like MeOH because it is harder to burn these fuels in a compression ignition engine due to high auto-ignition resistance.

Fig. 10 shows the combustion stability at the low load PPC operation of the MeOH fuelled engine. It is observed that the COV

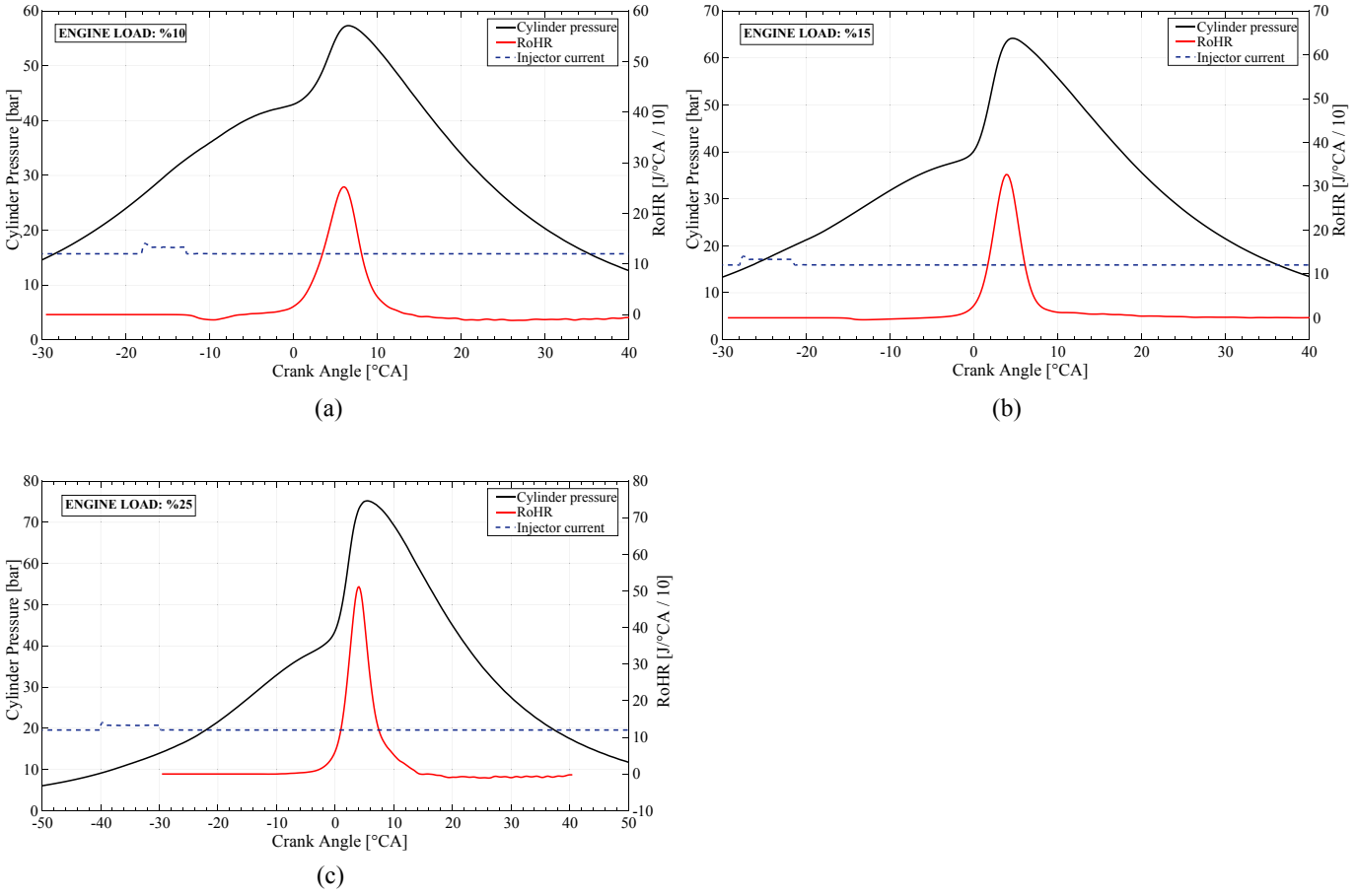

Fig. 9. In-cylinder pressure and RoHR curves at (a) %10 engine load, (b) %15 engine load, (c) %25 engine load.

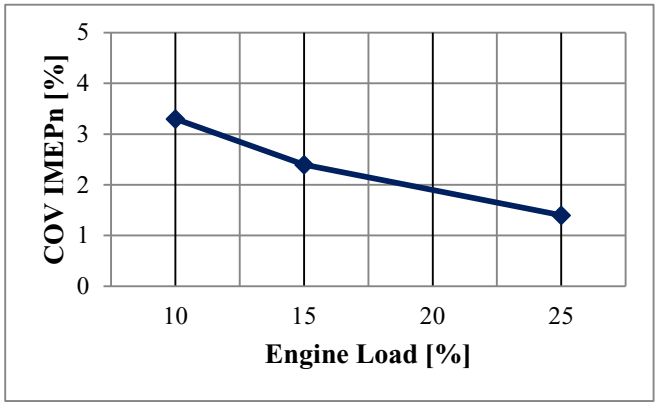

Fig. 10. MeOH fuelled engine stability at low loads.

$IMEP_n$ values are below 5%, which indicates the good stability of the combustion. Calculated COV $IMEP_n$ are 3.3%, 2.4%, and 1.4% for 10%, 15%, and 25% engine load, respectively. It is also observed that the COV $IMEP_n$ value decreases with the increase of the engine load. It is because; in-cylinder temperatures are lower at lower engine loads, which results in harder combustion of MeOH. It burns easier by the increase of the engine load and higher in-cylinder temperatures.

3.2.2. Maximum pressure rise rate

dP/dCAD is a value of the maximum pressure rise rate per crank angle degree. If this value is too high, it can give damage to the in-cylinder engine parts, and possible fatal problems can occur. In addition to the damage possibility, the engine works noisier with higher dP/dCAD. Fig. 11 shows the dP/dCAD with the ignition delay at low load PPC operation of the engine. The dP/dCAD is related to the ignition delay. Longer ignition delay forms a more homogenous mixture, which eliminates fuel-rich regions in the combustion chamber. This promotes the burning of the fuel, and it results in a higher pressure rise rate per crank angle. It can be seen in the figure that, the ignition delay increases from 20 CAD to 40 CAD, while dP/dCAD increases from 7.6 bar to 21.3 bar with higher engine load. The maximum pressure rise rate can be reduced by changing the start of injection (SOI) timing or using the split injection strategy rather than the single injection strategy. This investigation shows that the maximum pressure rise rate is high, but in safe limits at all low load operation.

3.2.3. In-cylinder and exhaust temperatures

Other important things for the stable working of the engine are in-cylinder and exhaust temperatures. As well as high in-cylinder and exhaust temperatures are harmful to the engine parts, especially for exhaust valves, low in-cylinder and exhaust temperatures are also harmful to the engine. Lower in-cylinder and exhaust temperatures can be observed at the low load operation of the engines. Low in-cylinder temperature is the cause of cold corrosion on the cylinder liner, and low exhaust temperature below 250 °C leads to cold corrosion and fouling at the exhaust pathways (MarineinSight, 2016). The cold corrosion happens when the liner temperatures are below the dew point, sulfur trioxide (SO_3) in a

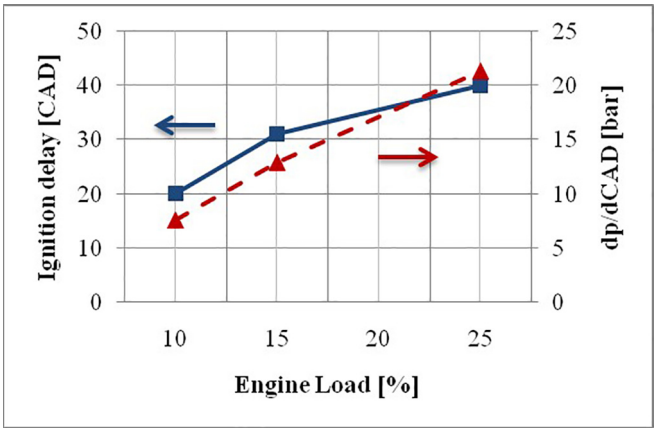

Fig. 11. Ignition delay and dP/dCAD at low load operation.

vapor phase starts to condense into a liquid phase, reacts with water and form sulfuric acid (H_2SO_4) on the liner (CIMAC, 2017). It can also happen at the exhaust pathway, and corrode metal surfaces. This reaction mostly happens during the continuous operation of the main engine at the low loads, the slow steaming operation is one of them. Fig. 12 shows the in-cylinder and exhaust temperatures of MeOH PPC at the low load operation of the engine. It can be seen that the exhaust temperatures are 211 °C, 248 °C and 330 °C, the in-cylinder average temperatures are 1518 °C, 1534 °C and 1611 °C, and the maximum in-cylinder temperatures are 2004 °C, 2105 °C and 2179 °C at 10%, 15% and 25% engine loads, respectively. A previous study showed that the exhaust receiver temperatures during the slow steaming operation of the conventional fuelled main engine were 304 °C and 329 °C at 15% and 25% engine loads, respectively (Guan et al., 2014). It is expected that the exhaust temperature is higher than the exhaust receiver temperature. The MeOH PPC operation results with reduced heat loss to the exhaust, which is consistent with the previous study (Shamun et al., 2018). The liner temperatures can be low and promote cold corrosion, particularly at 10% and 15% engine loads. However the exhaust temperature is lower than the cold corrosion limit at 10% engine load, and it is at the limit at 15% engine load, the MeOH has the advantage of sulfur-free structure, which does not form any sulfur trioxides and sulfuric acid reactions in the cylinder. In addition to the sulfur-free structure, the combustion of MeOH forms almost zero PM emissions even at the low load operation, which results in no fouling at in-cylinder components and exhaust pathways. This provides operation of the engine with lower exhaust temperature, which means less heat to the exhaust losses

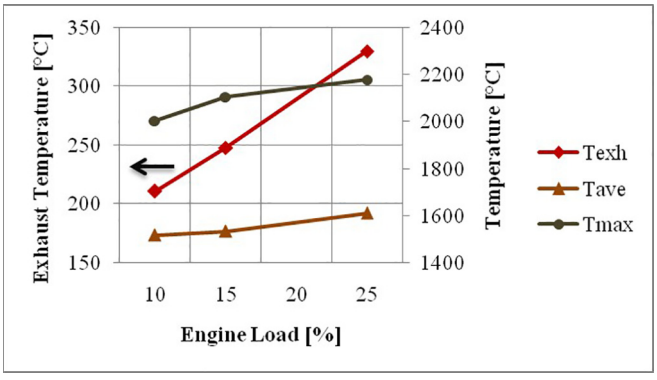

Fig. 12. Exhaust and in-cylinder temperatures at low load operation.

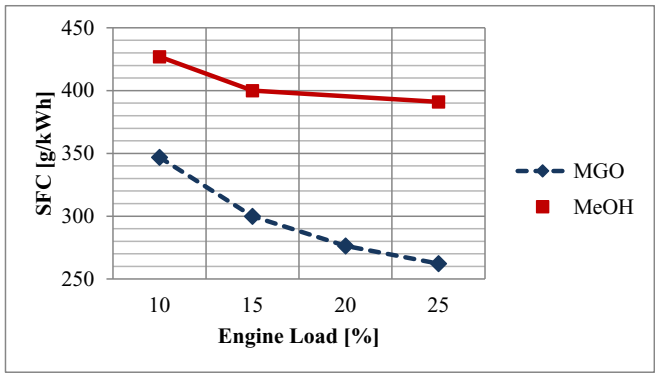

Fig. 13. SFC at the low load operation.

and higher engine efficiency.

3.2.4. Specific fuel consumption

The SFC values for the MeOH are measured at the experiments as 427 g/kWh, 400 g/kWh and 391 g/kWh for 10%, 15% and 25% engine loads, respectively. Fig. 13 shows the SFC of the MGO and MeOH at the low load operation. The MeOH fuel has higher SFC than the MGO, due to the low lower heating value (LHV) of the fuel. The MeOH has the LHV of 19.9 MJ/kg, while the MGO has the LHV of 42.8 MJ/kg (ETB, 2003). This is the downside of MeOH fuel when it is compared to conventional fuels. Fig. 14 shows specific energy consumption (SEC) of the MeOH and MGO fuelled engines. It can be seen in the figure that however, the MeOH consumption is higher than the MGO consumption for the loads, SEC is lower for the MeOH fuelled engine. It means less energy is needed for the engine work during the MeOH PPC low load operation of the diesel engine.

3.2.5. Engine efficiency

Fig. 15 shows the efficiencies of the engine at the low load MeOH PPC operation. It can be seen in the figure that the combustion efficiency increases from 0.94 to 0.99 from 10% to 15% engine load, and remains constant until 25% engine load. Lower combustion efficiency at 10% engine load can be occurred, due to low in-cylinder temperatures, which does not promote the combustion event. The thermodynamic efficiency is 0.45 at a 10% engine load, and rises to 0.47 at a 25% engine load, while the gross indicated efficiency is 0.42 at a 10% engine load, and rise to 0.46 at 25% engine load. Despite the low engine loads, the thermodynamic efficiency and gross indicated efficiency is high. This can be due to the high charge cooling effect, high charge density and low heat loss to the exhaust, lubricating oil and cooling water (Verhelst et al., 2019). In

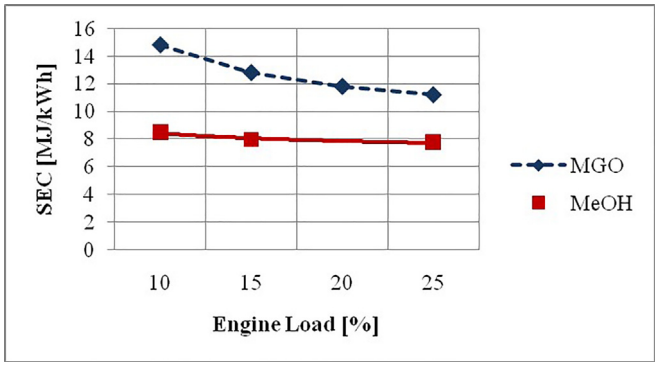

Fig. 14. SEC at the low load operation.

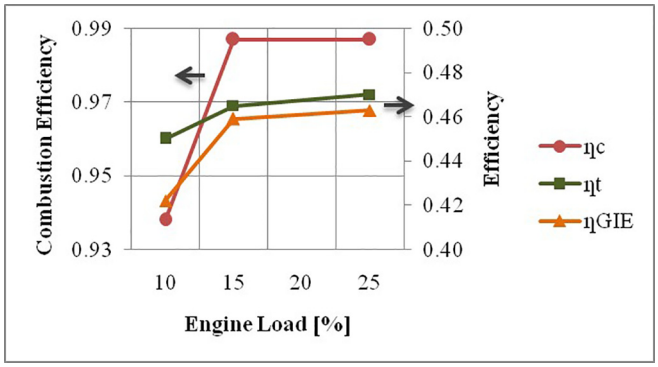

Fig. 15. Efficiencies at low loads with MeOH usage.

addition to this, high engine efficiency of the PPC concept is another reason for high efficiencies at the low loads (Benajes et al., 2014; Tuner et al., 2018).

It can be seen in Fig. 16 that the efficiency is extremely lower than the MeOH fuelled operation of the engine. The η_{GIE} is between 0.24 and 0.32 from 10% to 25% engine load. It is observed that using the MeOH PCC concept at the low load of the diesel engine has the engine efficiency advantage, which is consistent with previous low load PPC studies.

As a result of the operational performance investigation of the MeOH fuel, it can be said that this fuel can be used with the PPC concept at the low speed low-load operation of the main engine of the ships. The slow steaming approach or slow speed navigation at the strait and canal passages can be done with the MeOH fuel without any operational issues.

3.2.6. Economic performance

Fuel cost is a major parameter for the maritime trade, and the fuel expenses constitute 50–70% of the total operating expenses of a ship (Kim et al., 2016; Dere and Deniz, 2019). As a consequence, it will determine the tendency towards alternative fuel usage on ships. Fig. 17 compares the LSMGO and MeOH prices according to low price (LP) and high price (HP) scenarios. The fuel costs are calculated as a usd/kWh basis for each engine load in this study. The calculated and measured SFC values of the MGO and MeOH at each load are used at the calculations. The LP and HP values of the LSMGO are taken as 549.5 usd/MT and 616 usd/MT, respectively (Ship and Bunker, 2019), while the LP and HP values of the MeOH are taken as 345 usd/MT and 432 usd/MT, respectively (Methanex, 2019).

It is observed in the figure that the MeOH LP has lower usd/kWh value than both LSMGO scenarios, although the SFC of MeOH is

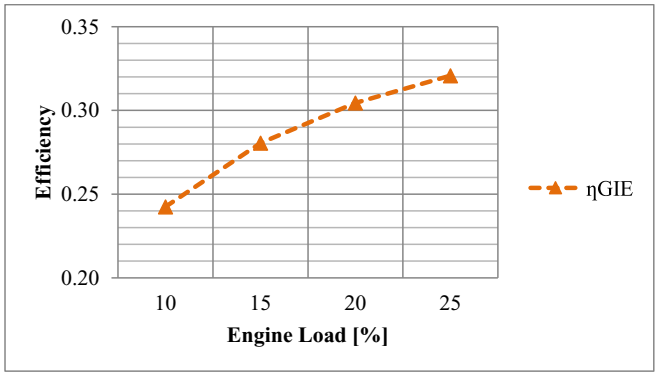

Fig. 16. Efficiency at low loads with MGO usage.

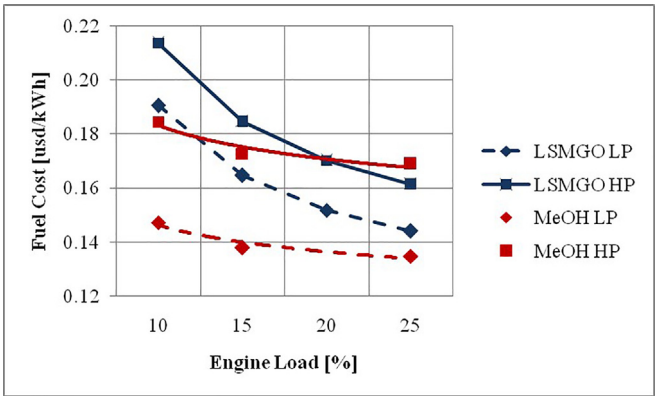

Fig. 17. Fuel cost versus engine load.

higher than the LSMGO, due to low LHV value. It is 0.147 usd/kWh, 0.138 usd/kWh and 0.135 usd/kWh at 10%, 15% and 25% engine loads, respectively. It is also seen that the gap between the MeOH LP and LSMGO LP scenarios reduces with the increase of the engine load from 10% to 25%. The MeOH HP scenario has a lower fuel cost than both LSMGO scenarios at 10% engine load with 0.184 usd/kWh, but it is higher than the LSMGO LP scenario at the remaining engine loads, while it is lower than the LSMGO HP scenario at 15% engine load, and almost similar with the LSMGO HP scenario at 20% and 25% engine loads. As a result of the investigation it is obvious that, if the MeOH LP scenario spreads worldwide, the MeOH will have a good advantage for onboard usage at the low load operation. But it is still competitive fuel with the MeOH HP scenario, because the low sulfur fuels are needed to be used for the upcoming maritime legislation, and the LSMGO is an expensive fuel in the current situation. The economic performance investigation corroborates with the previous study of Ellis and Tanneberger (2015).

According to the findings of the study, it is observed that the MeOH PPC concept emits low emissions of CO_2 and NO_X and zero emissions of SO_X and PM at slow speed low load operation of the engine. It complies with the international emission regulations. The operational performance shows that the MeOH PPC has good combustion stability, acceptable maximum pressure rise rate and in-cylinder temperatures, and higher engine efficiency than the conventional diesel combustion at the slow speed low load operation of the engine. The economic performance of the MeOH PPC is better or about the same with the conventional MGO operation. The results show that the MeOH PPC is a solution for the shipping emission effect on the coastal settlements while it does not increase the risk and expense of the engine operation on the ships.

4. Conclusion

In this paper, the operational, environmental and economic performance of methanol fuel under the low load PPC operation of the engine was investigated. The emissions, combustion properties, efficiency, specific fuel consumption and the fuel cost of the methanol at the low loads were highlighted in the study. Some of the main findings of the study were;

- The CO_2 emissions of the MeOH were lower than the MGO, despite the SFC of MeOH was higher. Low carbon content (0.375) of the MeOH is the reason for low CO_2 formation. The MeOH has an advantage at recent CO_2 emission mitigation legislations of IMO and EU.
- The NO_X emissions of the MeOH PPC complied with the limits of the IMO NO_X Tier III according to the experimental results. On

the other hand, the MGO did not comply with IMO NO_X Tier II limits and even it did not comply with IMO NO_X Tier I limits at 10% and 15% engine loads.

- The SO_X emissions of the MGO complied with the SO_X ECA limits according to the calculations, because the MGO was assumed as LSMGO (0.1% sulfur content) in this study. The MeOH is sulfur-free fuel, which is naturally SO_X ECA limit compliant fuel.
- The combustion stability investigation showed that the MeOH PPC engine had good combustion stability with the COV $IMEP_n$ below 5%. The MeOH fuel does not form any combustion issues like misfire events at the low load operation.
- The pressure rise rate was in acceptable limits, which cannot give any damage to the engine during operation. The in-cylinder and exhaust temperatures were low, especially at 10% and 15% engine loads. If the engine worked with conventional fuels, it would form cold corrosion and fouling inside the cylinder and at the exhaust pathways. But, thanks to the structure of the MeOH, it is sulfur-free fuel, which does not form sulfuric acid at the low in-cylinder and exhaust temperatures. In addition to this, almost zero PM emissions result with almost zero fouling in the cylinder or at the exhaust pathways.
- The MeOH PPC efficiencies were high with the combustion efficiency of 0.94–0.99, the thermodynamic efficiency of 0.45–0.47 and the gross indicated efficiency of 0.42–0.46 at the low load operation, while the MGO fuelled operation gross indicated efficiency was between 0.24 and 0.32.
- The fuel cost of the MeOH at the low price scenario was lower than the low price and high price scenarios of the MGO. If the MeOH price worldwide is as low as some areas in the world, the MeOH fuel usage on ships will spread widely. However the MeOH high price scenario has a high price, it is still competitive with the LSMGO prices worldwide.

The ship main engine can be considered as a production facility that converts the chemical energy of the fuels to the propulsion work. According to the findings of this study, the ship main engine will emit lesser emissions to the atmosphere and its efficiency will increase during the operation by using the MeOH PPC on ships. This will comply with the fundamentals of the 'Cleaner Production', which are preventing waste formation and increasing efficiency in the use of energy during the operation. However the MeOH PPC has promising results, there are barriers applying this concept on the ships. These barriers come from the fuel itself. The MeOH has half of the LHV of MGO, which means twice of the tank volume of MGO is needed. Additionally, the infrastructure of the bunkering facilities for the MeOH is low in number. This can limit the sailing distance of a ship. The MeOH is a low-flashpoint fuel and has a corrosive effect on some metal and plastic parts. Some of the ship main engine parts are needed to be changed with the MeOH compliant parts. As it was mentioned before, there are low numbers of MeOH fuelled ships in operation. For this reason, it is hard to find the MeOH compliant parts or the parts are expensive recently.

Despite there are barriers to use the MeOH PPC, it is not impossible to apply on the ships. The MeOH can be stored in double bottom tanks, which are forbidden for conventional fuels, provide an advantage over conventional fuels and can remove the requirement of higher tank volume need. The number of bunkering facilities can be increased, because the MeOH is one of the important substances for the chemical industry, and it has a huge amount of annual production in the worldwide. The MeOH compliant part prices can be reduced with the increased supply – demand balance. In addition to this less modification need on the engine, less initial costs for the system application than the after-treatment methods are other advantages of the MeOH PPC.

The future study will be the investigation of the effects of the MeOH PPC concept at the whole load range of the engine on engine performance and emissions. The results will be interpreted by taking into consideration of the maritime industry needs. It is expected that the MeOH fuel will show promising results at higher engine loads.

Acknowledgement

The authors wish to thank the Department of Energy Sciences, the division of Combustion Engines at Lund University to provide their laboratory and funding for the experimental part of this study.

List of nomenclature and abbreviations

aHRR	Apparent heat release rate
ATDC	After top dead center
BC	Black carbon
CA	Crank angle
CA50	the crank angle where half of the heat is released
CO	Carbon monoxide
CO_2	Carbon dioxide
COV $IMEP_n$	Coefficient of variation of net indicated mean effective pressure
Cp	Specific heat at constant pressure
Cv	Specific heat at constant volume
DISI	Direct injection spark ignition
dP/dCAD	Maximum pressure rise rate per crank angle degree
ECA	Emission Control Area
EEDI	Energy Efficiency Design Index
EEOI	Energy Efficiency Operational Indicator
EGR	Exhaust gas recirculation
EVO	Exhaust valve opening
FuelMEP	Fuel mean effective pressure
HCCI	Homogeneous charge compression ignition
HFO	Heavy fuel oil
HP	High price
H_2SO_4	Sulfuric acid
IMEP	Gross indicated mean effective pressure
$IMEP_n$	Net indicated mean effective pressure
IMO	International Maritime Organization
IVC	Intake valve closing
LHV	Lower heat value
LNG	Liquefied natural gas
LP	Low price
LPG	Liquefied petroleum gas
LSMGO	Low sulfur marine gas oil
MCR	Maximum continuous rating
MeOH	Methanol
MGO	Marine gas oil
MRV	Monitoring Reporting Verification
NO_X	Nitrogen oxides
ON	Octane number
QMEP	Heat mean effective pressure
PM	Particulate matter
PPC	Partially premixed combustion
RoHR	Rate of heat release
RO-RO	Roll on – roll of
r_c	Compression ratio
SCR	Selective catalytic reactor
SEEMP	Ship Energy Efficiency Management Plan
SEC	Specific energy consumption
SFC	Specific fuel consumption
SOI	Start of injection
SO_X	Sulfur oxide
SO_3	Sulfur trioxide

THC	Total hydrocarbons
UNCTAD	United Nations Conference on Trade and Development
V_d	Engine displacement volume
λ	Lambda
γ	The ratio of the specific heats
η_c	Combustion efficiency
η_{GIE}	Gross indicated efficiency
η_t	Thermodynamic efficiency

References

Ammar, N.R., 2018. Energy – and cost – efficiency analysis of greenhouse gas emission reduction using slow steaming of ships: case study RO-RO cargo vessel. Ships Offshore Struct. 13 (8), 868–876.

Ammar, N.R., 2019. An environmental and economical analysis of methanol fuel for a cellular container ship. Transport. Res. Part D 69, 66–76.

Ammar, N.R., Seddiek, I.S., 2017. Eco-environmental analysis of ship emission control methods: case study RO-RO cargo vessel. Ocean Eng. 137, 166–173.

An, Y., Jaasim, M., Raman, V., Im, H.G., Johansson, B., 2018. In-cylinder combustion and soot evolution in the transition from conventional compression ignition (CI) mode to partially premixed combustion (PPC) mode. Energy Fuels 2018, 2306–2320.

An, Y., Raman, V., Tang, Q., Shi, H., Sim, J., Chang, J., Magnotti, G., Johansson, B., 2019. Combustion stability study of partially premixed combustion with low-octane fuel at low engine load conditions. Appl. Energy 235, 56–67.

Baldi, F., Bengtsson, S., Andersson, K., 2013. The influence of propulsion system design on the carbon footprint of different marine fuels. In: Low Carbon Shipping Conference. London 2013.

Benajes, J., Molina, S., Novella, R., De Lima, D., 2014. Implementation of the partially premixed combustion concept in a 2-stroke HSDI diesel engine fueled with gasoline. Appl. Energy 122, 94–111.

Brynolf, S., Fridell, E., Andersson, K., 2014. Environmental assessment of marine fuels: liquefied natural gas, liquefied biogas, methanol and bio-methanol. J. Clean. Prod. 74, 86–95.

Cariou, P., 2011. Is slow steaming a sustainable means of reducing CO_2 emissions from container shipping? Transport. Res. Part D 16, 260–264.

Chatzinikolaou, S.D., Oikonomou, S.D., Ventikos, N.P., 2015. Health externalities of ship air pollution at port – piraus port case study. Transport. Res. Part D 40, 155–165.

Corbett, J.J., Wang, H., Winebrake, J.J., 2009. The effectiveness and costs of speed reductions on emissions from international shipping. Transport. Res. Part D 14, 593–598.

Deniz, C., Durmusoglu, Y., 2008. Estimating shipping emissions in the region of the Sea of Marmara, Turkey. Sci. Total Environ. 390, 255–261.

Deniz, C., Kilic, A., 2010. Estimation and assessment of shipping emissions in the region of Ambarli Port, Turkey. Environ. Prog. Sustain. Energy 29, 107–115.

Deniz, C., Zincir, B., 2016. Environmental and economical assessment of alternative marine fuels. J. Clean. Prod. 113, 438–449.

Dere, C., Deniz, C., 2019. Load optimization of central cooling system pumps of a container ship for the slow steaming conditions to enhance the energy efficiency. J. Clean. Prod. 222, 206–217.

DNV, G.L., 2016. EU MRV Regulation. Date of access: 15/02/2019. https://www.dnvgl.com/maritime/eu-mrv-regulation/index.html.

Dragovic, B., Tzannatos, E., Tselentis, V., Mestrovic, R., Skuric, M., 2018. Ship emissions and their externalities in cruise ports. Transport. Res. Part D 61, 289–300.

EEA, 2000. Analysis of Commercial Marine Vessels Emissions and Fuel Consumption Data. Office of Transportation and Air Quality. U.S. Environmental Protection Agency. EPA420-R-00-002.

Ellis, J., 2017. Methanol – an Alternative Fuel for Shipping?, Workshop: Marine Fuels beyond LNG – Methanol as an Alternative? Elsfleth, 7 June 2017.

Ellis, J., Tanneberger, K., 2015. Study on the Use of Ethyl and Methyl Alcohol as Alternative Fuels in Shipping. Report prepared for the European Maritime Safety Agency (EMSA). Final report version 20151204.5. SSPA Project number: 20157412.

Engineering Toolbox (ETB), 2003. Fuels – higher and lower calorific values. Date of access: 13/02/2019. https://www.engineeringtoolbox.com/fuels-higher-calorific-values-d_169.html.

Fan, Y.V., Perry, S., Klemes, J.J., Lee, C.T., 2018. A review on air emissions assessment: transportation. J. Clean. Prod. 194, 673–684.

Gilbert, P., Walsh, C., Traut, M., Kesieme, U., Pazouki, K., Murphy, A., 2018. Assessment of full life-cycle air emissions of alternative shipping fuels. J. Clean. Prod. 172, 855–866.

Global Combustion Systems (GCS), 2019. Oil Fuel Properties. Date of Access: 21/05/2019. http://www.globalcombustion.com/oil-fuel-properties/.

Gong, C., Peng, L., Chen, Y., Liu, J., Liu, F., Han, Y., 2018. Computational study of intake temperature effects on mixture formation, combustion and unregulated emissions of a DISI methanol engine during cold start. Fuel 234, 1269–1277.

Guan, C., Theotokatos, G., Zhou, P., Chen, H., 2014. Computational investigation of a large containership propulsion engine operation at slow steaming conditions. Appl. Energy 130, 370–383.

Han, X., Yang, Z., Wang, M., Tjong, J., Zheng, M., 2017. Clean combustion of n-butanol as a next generation biofuel for diesel engines. Appl. Energy 198, 347–359.

Heywood, J.B., 1988. Internal Combustion Engine Fundamentals. McGraw-Hill Education.

ICF, 2009. Current Methodologies in Preparing Mobile Source Port-Related Emission Inventories. U.S. Environmental Protection Agency.

International Maritime Organization (IMO), 2011. Resolution MEPC.203(62), Annex 19, Adopted on 15 July 2011. Amendments to the Annex of the Protocol of 1997 to Amend the International Convention for the Prevention of Pollution from Ships, 1973, as Modified by the Protocol of 1978 Relating Thereto (Inclusion of Regulations on Energy Efficiency for Ships in MARPOL Annex VI).

International Maritime Organization (IMO), 2014. IMO GHG Study 2014.

International Maritime Organization (IMO), 2019a. Emission control areas designated under MARPOL Annex VI. Date of access: 15/02/2019. http://www.imo.org/en/OurWork/Environment/PollutionPrevention/AirPollution/Pages/Emission-Control-Areas-(ECAs)-designated-under-regulation-13-of-MARPOL-Annex-VI-(NOx-emission-control (aspx>).

International Maritime Organization (IMO), 2019b. Data collection system for fuel oil consumption os ships. Date of access: 15/02/2019. http://www.imo.org/en/ourwork/environment/pollutionprevention/airpollution/pages/data-collection-system.aspx.

International Maritime Organization (IMO), 2019c. Nitrogen Oxides – Regulation 13. Date of Access: 15/02/2019. http://www.imo.org/en/ourwork/environment/pollutionprevention/airpollution/pages/nitrogen-oxides-(nox)-%E2%80%93-regulation-13.aspx.

International Maritime Organization (IMO), 2019d. Sulfur Oxides and Particulate Matter – Regulation 14. Date of access: 15/02/2019. http://www.imo.org/en/OurWork/Environment/PollutionPrevention/AirPollution/Pages/Sulphur-oxides-(SOx)-%E2%80%93-Regulation-14.aspx.

International Council on Combustion Engines, CIMAC, 2017. Guideline Cold Corrosion in Marine Two Stroke Engines, vol. 11, 2017.

Jafarzadeh, S., Schjølberg, I., 2018. Operational profiles of ships in Norwegian waters: an activity-based approach to assess the benefits of hybrid and electric propulsion. Transport. Res. Part D 65, 500–523.

Jain, A., Singh, A.P., Agarwal, A.K., 2017. Effect of fuel injection parameters on combustion stability and emissions of a mineral diesel fueled partially premixed charge compression. Appl. Energy 190, 658–669.

Janssen, N.A., Gerlofs-Nijland, M.E., Lanki, T., Salonen, R.O., Cassee, F., Hoek, G., Fischer, P., Brunekreef, B., Krzyzanowski, M., 2012. World Health Organization, Health Effects of Black Carbon.

Jensen, M.C., Jakobsen, S.B., 2009. MAN B&W Service Letter SL09-511/MTS, Low Load Operation 10% to 40% Engine Load.

Kim, J., Kim, H., Jun, H., Kim, C., 2016. Optimizing ship speed to minimize total fuel consumption with multiple time windows. Hindawi Publishing Corporation. Math. Probl. Eng. 2016 https://doi.org/10.1155/2016/3130291.

Klaus, O.L., Villetti, L., Siqueira, J.A.C., De Souza, S.N.M., Santos, R.F., Nogueira, C.E.C., Rosseto, C., 2013. Efficiency and fuel specific consumption of an engine running on fish biodiesel. Sci. Res. Essays 8 (42), 2120–2122. https://doi.org/10.5897/SRE2013.5550.

Leermakers, C.A.J., Bakker, P.C., Nijssen, B.C.W., Somers, L.M.T., Johansson, B.H., 2014. Low octane fuel composition effects on the load range capability of partially premixed combustion. Fuel 135, 210–222.

Lindstad, H., Asbjornslett, B.E., Stromman, A.H., 2011. Reductions in greenhouse gas emissions and cost by shipping at lower speeds. Energy Policy 39, 3456–3464.

MAN, PrimeServ, 2012. Slow Steaming, Benefiting Retrofit Solutions from MAN PrimeServ. Technical paper, September 2012.

Mao, B., Liu, H., Zheng, Z., Yao, M., 2018. Influence of fuel properties on multi-cylinder PPC operation over a wide range of EGR and operating conditions. Fuel 215, 352–362.

Maragkogianni, A., Papaefthimiou, S., 2015. Evaluating the social cost of cruise ships air emissions in major ports of Greece. Transport. Res. Part D 36, 10–17.

MarineinSight, 2016. How to Tackle Low Load Operating Conditions of Marine Engine? Date of access: 10/02/2019. https://www.marineinsight.com/case-studies/how-to-tackle-low-load-operating-conditions-of-marine-propulsion-engine/.

Merico, E., Gambaro, A., Argiriou, A., Alebic-Juretic, A., Barbaro, E., Cesari, D., Chasapidis, L., Dimopoulos, S., Dinoi, A., Donateo, A., Giannaros, C., Gregoris, E., Karagiannidis, A., Konstandopoulos, A.G., Ivosevic, T., Liora, N., Melas, D., Mifka, B., Orlic, I., Poupkou, A., Sarovic, K., Tsakis, A., Giua, R., Pastore, T., Nocioni, A., Contini, D., 2017. Atmospheric impact of ship traffic in four Adriatic-Ionian port-cities: comparison and harmonization of different approaches. Transport. Res. Part D 50, 431–445.

Methanex, 2019. Methanol Price Sheet. Date of Access: 11/02/2019. https://www.methanex.com/sites/default/files/methanol-price/Mx-Price-Sheet%20-%20Jan%2029%2C%202019.pdf.

Naser, N., Jaasim, M., Atef, N., Chung, S.H., Im, H.G., Sarathy, S.M., 2017. On the effects of fuel properties and injection timing in partially premixed compression ignition of low octane fuels. Fuel 207, 373–388.

Norlund, E.K., Gribkovskaia, I., 2013. Reducing emissions through speed optimization in supply vessel operations. Transport. Res. Part D 23, 105–113.

Pan, W., Yao, C., Han, G., Wei, H., Wang, Q., 2015. The impact of intake air temperature on performance and exhaust emissions of a diesel methanol dual fuel engine. Fuel 162, 101–110.

Przybyla, G., Postrzednik, S., Zmudka, Z., 2016. The impact of air-fuel mixture composition on SI engine performance during natural gas and producer gas combustion. IOP Conf. Ser. Mater. Sci. Eng. 148 (1), 12082. September 2016.

Shahhosseini, H.R., Iranshahi, D., Saeidi, S., Pourazadi, E., Klemes, J.J., 2018. Multi-objective optimization of steam methane reforming considering stoichiometric ratio indicator for methanol production. J. Clean. Prod. 180, 655–665.

Shamun, S., 2019. Characterization of the Combustion of Light Alcohols in CI Engines, Performance, Combustion Characteristics and Emissions. Dissertation thesis. Division of Combustion Engines, Department of Energy Sciences, Lund University.

Shamun, S., Shen, M., Johansson, B., Tuner, M., et al., 2016. Exhaust PM analysis of alcohol fueled heavy-duty engine utilizing PPC. SAE Int. J. Engines 9 (4). https://doi.org/10.4271/2016-01-2288, 2016.

Shamun, S., Novakovic, M., Malmborg, V.B., Preger, C., Shen, M., Messing, M.E., Pagels, J., Tuner, M., Tunestal, P., 2017. Detailed Characterization of Particulate Matter in Alcohol Exhaust Emissions. 9th International Conference on Modeling and Diagnostics for Advanced Engine Systems, vol. 2017. COMODIA, Okayama, Japan, pp. 25–28. https://doi.org/10.1299/jmsesdm.2017.9.B304. July 2017.

Shamun, S., Zincir, B., Shukla, P., Valladolid, P.G., Verhelst, S., Tuner, M., 2018. Quantification and analysis of the charge cooling effect of methanol in a compression ignition engine utilizing PPC strategy. In: Proceedings of the ASME 2018, Internal Combustion Engine Division Fall Technical Conference. ICEF2018, 4-7 November 2018, San Diego, CA, USA.

Ship, Bunker, 2019. World Bunker Prices. https://shipandbunker.com/prices. Date of Access: 11/02/2019.

Sjöberg, M., Dec, J., 2003. Combined effects of fuel-type and engine speed on intake temperature requirements and completeness of bulk-gas reactions for HCCI combustion. SAE Technical Paper 2003-01-3173, 2003. Doi:10/4271/2003-01-3173.

Styhre, L., Winnes, H., Black, J., Lee, J., Le-Griffin, H., 2017. Greenhouse gas emissions from ships in ports – case studies in four continents. Transport. Res. Part D 54, 212–224.

Tezdogan, T., Demirel, Y.K., Kellett, P., Khorasanchi, M., Incecik, A., Turan, O., 2015. Full-scale unsteady RANS CFD simulations of ship behavior and performance in head seas due to slow steaming. Ocean Eng. 97, 186–206.

Tezdogan, T., Incecik, A., Turan, O., Kellett, P., 2016. Assessing the impact of a slow steaming approach on reducing the fuel consumption of a containership advancing in head seas. Transportation Research Procedia 14, 1659–1668.

Tuner, M., 2016. Review and benchmarking of alternative fuels in conventional and advanced engine concepts with emphasis on efficiency, CO_2, and regulated emissions. SAE Technical Paper 2016-01-0882. https://doi.org/10.4271/2016-01-0882.

Tuner, M., Aakko-Saksa, P., Molander, P., 2018. SUMMETH – Sustainable Marine Methanol Deliverable D3.1 Engine Technology, Research, and Development for Methanol in Internal Combustion Engines. Final Report.

United Nations Conference on Trade and Development (UNCTAD), 2018. Review of Maritime Transport 2018.

Verhelst, S., Turner, J.W.G., Sileghem, L., Vancoillie, J., 2019. Methanol as a fuel for internal combustion engines. Prog. Energy Combust. Sci. 70, 43–88.

Wang, S., van der Waart, K., Somers, B., de Goey, P., 2017. Experimental study on the potential of higher octane fuels for low load partially premixed combustion. SAE Technical Paper 2017-01-0750. https://doi.org/10.4271/2017-01-0750, 2017.

Wei, L., Yao, C., Wang, Q., Pan, W., Han, G., 2015. Combustion and emission characteristics of a turbocharged diesel engine using high premixed ratio of methanol and diesel fuel. Fuel 140, 156–163.

Yao, C., Pan, W., Yao, A., 2017. Methanol fumigation in compression-ignition engines: a critical review of recent academic and technological developments. Fuel 209, 713–732.

Yin, L., Turesson, G., Tunestal, P., Johansson, R., 2019a. Evaluation and transient control of an advanced multi-cylinder engine based an partially premixed combustion. Appl. Energy 233–234, 1015–1026.

Yin, L., Lundgren, M., Wang, Z., Stamatoglou, P., Richter, M., Andersson, Ö., Tunestal, P., 2019b. High efficient internal combustion engine using partially premixed combustion with multiple injections. Appl. Energy 233–234, 516–523.

Zincir, B., Deniz, C., 2018. Maritime industry developments related to alternative fuels. In: INT-NAM 2018, 3rd International Naval Architecture and Maritime Symposium, pp. 24–25. April 2018, Istanbul, Turkey.